

Purification, crystallization and preliminary X-ray crystallographic analysis of recombinant murine Golgi mannosidase IA, a class I α -mannosidase involved in Asn-linked oligosaccharide maturation

Francois Vallée,^a Anita Lal,^b
Kelley W. Moremen^a and
P. Lynne Howell^{a,c*}

^aStructural Biology and Biochemistry, Research Institute, Hospital for Sick Children, 555 University Avenue, Toronto, M5G 1X8, Ontario, Canada, ^bDepartment of Biochemistry and Molecular Biology and the Complex Carbohydrate Research Center, University of Georgia, Athens, GA 30602, USA, and ^cDepartment of Biochemistry, Faculty of Medicine, University of Toronto, Toronto, M5S 1A8, Ontario, Canada

Correspondence e-mail: howell@sickkids.on.ca

Golgi mannosidase IA is a class I α -mannosidase which catalyzes the conversion of Man₉GlcNAc₂ or Man₈GlcNAc₂ oligosaccharide substrates to Man₅GlcNAc₂ during the maturation of Asn-linked oligosaccharides. The enzyme is a type II membrane protein, and a recombinant form of mannosidase IA from mouse, lacking the transmembrane domain, has been expressed in *Pichia pastoris*, purified to homogeneity and crystallized by the hanging-drop vapor-diffusion method. The crystals grow as thin rods, with unit-cell dimensions $a = 54.9$, $b = 135.01$, $c = 69.9$ Å. The crystals exhibit the symmetry of space group $P222_1$ and diffract to 2.8 Å resolution. The asymmetric unit contains one monomer (~53 kDa) and has a solvent content of 59%.

Received 22 May 1998

Accepted 28 September 1998

1. Introduction

α 1,2-Mannosidases are essential for the maturation of asparagine-linked oligosaccharides in mammalian cells. A precursor oligosaccharide (Glc₃Man₉GlcNAc₂) is assembled in the endoplasmic reticulum (ER) on the lipid carrier dolichol pyrophosphate and subsequently transferred to an asparagine residue within the tripeptide Asn-X-Ser/Thr sequence of the nascent polypeptide chain (reviewed in Kornfeld & Kornfeld, 1985). The precursor is processed during the passage through the ER and Golgi by the concerted action of α -glycosidases I and II, which remove the glucose residues, and a collection of processing α -mannosidases, which trim the α 1,2-linked mannose residues. The resulting oligosaccharide is the substrate for GlcNAc transferase I and subsequently α -mannosidase II, which cleaves two more mannose residues. In the last step of oligosaccharide maturation, the resulting GlcNAcMan₃GlcNAc₂ is modified by glycosyltransferases to yield a variety of complex oligosaccharide chains (Herscovics & Orlean, 1993; Kornfeld & Kornfeld, 1985; Moremen *et al.*, 1994).

Mammalian systems express several processing α -mannosidases which differ in their properties, subcellular locations and substrate and inhibitor specificities (for reviews, see Herscovics, 1998; Moremen *et al.*, 1994). On the basis of protein-sequence homologies, these enzymes and those from yeast and other species have been classified into two distinct classes: class I and class II mannosidases. The first class encompasses the α 1,2-mannosidases from mammals, yeast, *Aspergillus* and *Penicillium* which encode polypeptides of 63–73 kDa. These proteins are

typically Ca²⁺-dependent, are inhibited by 1-deoxymannojirimycin but not by swainsonine and act in the ER and Golgi (Moremen *et al.*, 1994). The second class is more heterogeneous and contains enzymes that can cleave α 1,2-, α 1,3- or α 1,6-linked mannose residues from the oligosaccharide. This class includes Golgi α -mannosidase II, a lysosomal acidic α -mannosidase and the mammalian cytosolic/ER α -mannosidase (Moremen *et al.*, 1994). These enzymes are 107–136 kDa in length, are inhibited by swainsonine and can use aryl glycosides as substrates. There is no sequence similarity between the two classes of proteins, and it has been shown that the two classes use different mechanisms for sugar cleavage (Howard *et al.*, 1997; Lal *et al.*, 1999; Lipari *et al.*, 1995), indicating that the two classes of enzymes have different three-dimensional structures.

Class I α 1,2 mannosidases are all type II membrane proteins with a short cytoplasmic tail, single transmembrane domain and a large COOH-terminal luminal catalytic domain. Several mammalian class I α 1,2 mannosidases have been cloned, including those from rabbit, human and mouse (Herscovics, 1998; Moremen *et al.*, 1994). In mouse tissues, two distinct class I α -mannosidase cDNA products were identified using a degenerate PCR approach and were shown to be encoded by different genes, indicating the existence of a mannosidase gene family. Comparison of these two highly homologous α 1,2-mannosidases, mannosidase IA (Lal *et al.*, 1994) and mannosidase IB (Herscovics *et al.*, 1994), has shown that they exhibit 67% sequence identity and that they have distinct preferential pathways for the cleavage of Man₉GlcNAc₂ to Man₅GlcNAc₂ (Lal *et al.*, 1999). Both murine

enzymes preferentially cleave three of the four α 1,2-linked mannose residues from $\text{Man}_9\text{GlcNAc}_2$, but one of the α 1,2-mannose residues is relatively resistant to digestion. These studies concluded that the *in vivo* substrates for these enzymes are likely to be a distinct $\text{Man}_8\text{GlcNAc}_2$ isomer (isomer Man8B) rather than $\text{Man}_9\text{GlcNAc}_2$ (Lal *et al.*, 1999; see Fig. 1).

An enzyme activity that was complementary to the murine Golgi mannosidases IA and IB was detected in an endoplasmic reticulum-enriched membrane fraction from rat liver, which was shown to cleave a single mannose residue from $\text{Man}_9\text{GlcNAc}_2$ to yield the Man8B isomer structure that is a substrate for mannosidases IA and IB (Lal *et al.*, 1999). Although a yeast enzyme with a similar specificity for the cleavage of $\text{Man}_9\text{GlcNAc}_2$ to the same $\text{Man}_8\text{GlcNAc}_2$ isomer has been cloned (Camirand *et al.*, 1991), characterized (Lal *et al.*, 1999; Lipari *et al.*, 1995; Lipari & Herscovics, 1996) and crystallized (Dole *et al.*, 1997), the mammalian equivalent of this enzyme has been neither purified nor cloned.

Since trimming reactions play a crucial role in the elaboration of biologically active glycoproteins, and the inhibition of this part of the processing pathway affects important cellular recognition processes such as angiogenesis, neutrophil adhesion to endothelial cells and natural-killer cell targeting (Ahrens, 1993; Nguyen *et al.*, 1993; Sriram Rao *et al.*, 1993), it is evident that the elucidation of the three-dimensional structure of a member of this class of enzymes is extremely important. We report here the successful crystallization and the preliminary X-ray characterization of the catalytic domain of recombinant murine mannosidase IA. This is the first step towards a structural comparison of the murine and yeast α 1,2 mannosidases. The crystallization of the yeast α 1,2 mannosidase has previously been reported (Dole *et al.*, 1997). Structural comparison of the two enzymes will reveal the similarities in the mechanisms of action for the two proteins and the factors which control the differences in specificity (*i.e.* the number and position of the saccharides cleaved by each enzyme).

2. Expression and purification

In order to obtain sufficient quantities of the protein for X-ray crystallographic studies, we have developed a large-scale expression and purification procedure. The murine Golgi processing mannosidase IA coding region (Lal *et al.*, 1994) was subcloned into the fungal expression vector pHIL S1 and transformed into the *his4 Pichia pastoris* host strain GS115 as previously described (Lal *et al.*, 1999). The transformant which expressed the highest level of secreted mannosidase activity in 11 shake-flask cultures was selected for larger scale fermentor culture. A saturated 1 l shake-flask culture of the mannosidase IA *P. pastoris* transformant in BMGY medium was used to inoculate a 20 l fermentor culture (20 l W. B. Moore fermenter at the Fermentation Research Facility, University of Georgia) in BMGY medium and the culture was incubated at 302 K with an agitation of 250 rev min^{-1} and an air flow of 12 l min^{-1} until the OD_{600} reached 24. Mannosidase IA expression was then induced by adding 50% (*v/v*) methanol to a final concentration of 0.5% to the culture medium once every 24 h. The media was harvested 168 h post-induction by methanol and the medium was clarified by centrifugation at 10000g for 60 min. The medium was filtered using a 0.45 μm filter and the supernatant was concentrated using a Pellicon ultrafiltration system, using a PLTK 30 kDa cutoff regenerated cellulose Pellicon 2 cassette filter (Millipore) to bring the volume down to 1 l. 4 l of 20 mM HEPES/NaOH pH 6.0 was added to the concentrated medium and it was concentrated further to 600 ml. Following the concentration step, the tangential-flow membrane cassette was washed with an additional 500 ml of 20 mM HEPES/NaOH buffer and this wash was pooled with the concentrated media sample for further purification. The concentrated media (1.1 l) was processed for purification by chromatography in five equal aliquots. The procedure used was essentially the same as described previously (Lal *et al.*, 1999) with the following modifications. The sizes of the Q-Sepharose Fast Flow column

Table 1

Diffraction data statistics.

Number of measured reflections	38583
Number of independent reflections	12836
Number of crystals	1
Resolution \dagger (Å)	2.8
$R_{\text{sym}}\ddagger$	11.0 (30.9)
Completeness	95.1 (92.1)
Crystal mosaicity	0.12
Average $I/\sigma(I)$	6.7

\dagger Resolution limit is defined as the limit beyond which fewer than 45% of the reflections have $I > 3\sigma(I)$. \ddagger Defined as $R_{\text{sym}} = \sum [I(k) - \langle I \rangle] / \sum I(k)$, where $I(k)$ and $\langle I \rangle$ represent the diffraction intensity values of the individual measurements and the corresponding mean values. The summation is over all measurements.

(25 \times 440 mm), the phenyl-Sepharose column (25 \times 150 mm) and the Cibacron Blue A dye column (15 \times 230 mm) were larger, but the buffers and the flow rates used were identical to those described for the small-scale purification. However, the washes were longer and the gradients were extended over a longer period. In addition, the mannosidase IA fractions pooled after the Cibacron Blue A dye column were processed through an additional gel-permeation chromatography step. The pooled fractions from the Cibacron Blue A dye column were concentrated by ultrafiltration through a YM-30 membrane. The concentrated mannosidase IA was diluted fivefold in 20 mM MES pH 6.5, 150 mM NaCl, 5 mM CaCl_2 and reconcentrated. This dilution and concentration procedure was repeated three times. The final volume was reduced to 6 ml and loaded at a flow rate of 1 ml min^{-1} onto a Superdex 200 column (16 \times 600 mm, Pharmacia) pre-equilibrated in 20 mM MES pH 6.5, 150 mM NaCl, 5 mM CaCl_2 , and the column was eluted in the same buffer. Fractions containing α -mannosidase activity were pooled and aliquots were subjected to SDS-PAGE. Fractions containing mannosidase IA were pooled, concentrated to 7.2 mg ml^{-1} using a Centricon 30 ultrafiltration membrane (Amicon) and were subsequently stored at 277 K prior to use in the crystallization trials.

3. Crystallization

Initial screening for crystallization conditions was performed using a sparse-matrix screen (Jancarik & Kim, 1991) at room temperature (293 K). All crystals were grown using the hanging-drop vapor-diffusion technique by mixing 2.5 μl of the protein solution with 2.5 μl of the precipitant on a siliconized glass cover slip and equili-

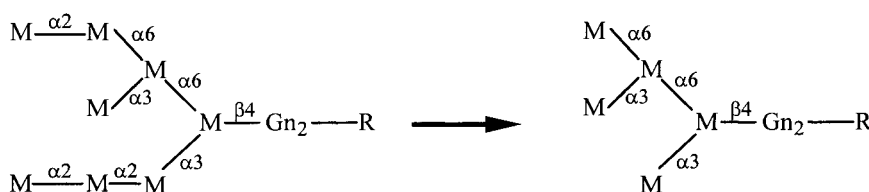


Figure 1

Catalytic activity of mouse mannosidase IA. M, mannose; Gn, *N*-acetyl glucosamine; R, protein.

brating the drop against 0.5 ml of the same precipitant solution. Small microcrystals grew within 2 d from a precipitant solution containing 30% PEG 4000, 200 mM lithium sulfate, 100 mM Tris-HCl buffer pH 8.5. Variation in the concentration of PEG (20–25%) and lithium sulfate (250 mM) resulted in larger crystals, which reached a maximal

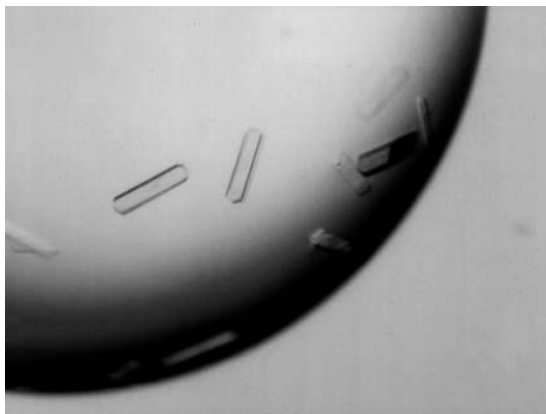


Figure 2
Crystals of mouse mannosidase IA. The crystals are approximately $0.4 \times 0.1 \times 0.05$ mm.

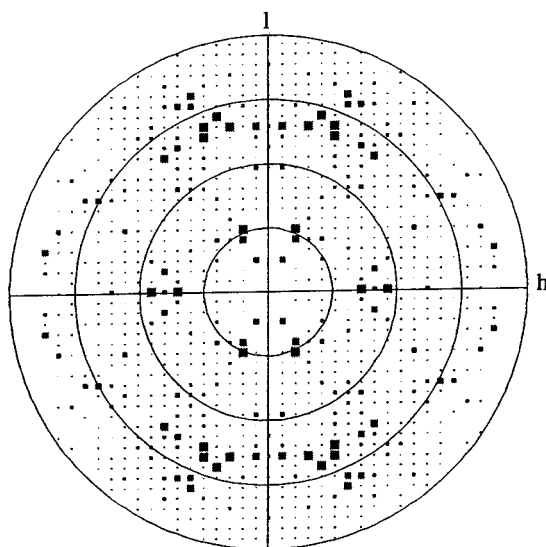


Figure 3
Pseudo-precession image of the $h0l$ zone of the reciprocal lattice displayed using the program *HKLVIEW* (Collaborative Computational Project, Number 4, 1994). The directions of the h and l axes are indicated on the diagram. Each reflection is represented by a square whose size depends on the amplitude of the reflection. The outer resolution limit corresponds to 2.8 Å resolution.

size of $0.1 \times 0.2 \times 0.4$ mm within 5 d (see Fig. 2).

4. X-ray analysis

The crystals were mounted in a quartz capillary and data were collected at room temperature on the Brandeis CCD detector at Station X12-C at the National Synchrotron Light Source, Brookhaven National Laboratory, NY, USA. The X-ray beam was monochromated to 1.00 Å by a Si(111) monochromator system. A total of 57 φ -scanning oscillation exposures in steps of 2° were recorded. Preliminary autoindexing to obtain cell parameters and the refinement of the cell and setting parameters were performed using the program *DENZO* (Otwinowski & Minor, 1997). The unit-cell dimensions were found to be $a = 54.9$, $b = 135.1$, $c = 69.9$ Å, $\alpha = \beta = \gamma = 90^\circ$. Reflections of the type $00l$ were found to be systematically absent for $l = 2n + 1$ reflections (see Fig. 3), uniquely determining the space group to be $P222_1$. On the basis of density calculations ($V_m = 2.44$ Å³ Da⁻¹; Matthews, 1968) we estimate that one molecule (~ 53 kDa) is present in the asymmetric unit. Since the protein requires Ca²⁺ for activity, the ability to replace the Ca²⁺ with holmium or ytterbium (A. Lal and K. W. Moremen, unpublished results) is being exploited in order to determine the structure of the protein using the multiple-wavelength anomalous diffraction method (Hendrickson, 1991).

We are grateful to Patrick Yip for technical assistance. This research is supported by grants from the National Institutes of

Health (RR05351 to KWM and GM46533 to KWM and PLH), and a grant from the Natural Sciences and Engineering Research Council of Canada to PLH. Diffraction data for this study were collected at Station X12-C, NSLS, Brookhaven National Laboratory. This facility is supported by the US Department of Energy Offices of Health and Environmental Research and Basic Energy Science and by the National Science Foundation.

References

- Ahrens, P. B. (1993). *J. Biol. Chem.* **268**, 385–391.
- Camirand, A., Haysen, A., Grondin, B. & Herscovics, A. (1991). *J. Biol. Chem.* **266**(23), 15120–15127.
- Collaborative Computational Project, Number 4 (1994). *Acta Cryst.* **D50**, 760–763.
- Dole, K., Lipari, F., Herscovics, A. & Howell, P. L. (1997). *J. Struct. Biol.* **120**, 69–72.
- Hendrickson, W. A. (1991). *Science*, **254**, 51–58.
- Herscovics, A. (1998). In *Comprehensive Natural Products Chemistry*, edited by B. M. Pinto. Amsterdam: Elsevier.
- Herscovics, A. & Orlean, P. (1993). *FASEB J.* **7**(6), 540–550.
- Herscovics, A., Schneikert, J., Athanassiadis, A. & Moremen, K. W. (1994). *J. Biol. Chem.* **269**(13), 9864–9871.
- Howard, S., Braum, C., McCarter, J., Moreman, K., Liao, Y.-F. & Withers, S. G. (1997). *Biochem. Biophys. Res. Commun.* **238**, 896–898.
- Jancarik, J. & Kim, S.-H. (1991). *J. Appl. Cryst.* **24**, 409–411.
- Kornfeld, R. & Kornfeld, S. (1985). *Annu. Rev. Biochem.* **54**, 631–664.
- Lal, A., Pang, P. S. K., Romero, P. A., Herscovics, A. & Moremen, K. W. (1999). *Glycobiology*. In the press.
- Lal, A., Schutzbach, J. S., Forsee, W. T., Neame, P. J. & Moremen, K. W. (1994). *J. Biol. Chem.* **269**(13), 9872–9881.
- Lipari, F., Gour Salin, B. J. & Herscovics, A. (1995). *Biochem. Biophys. Res. Commun.* **209**, 322–326.
- Lipari, F. & Herscovics, A. (1996). *J. Biol. Chem.* **271**(44), 27615–27622.
- Matthews, B. W. (1968). *J. Mol. Biol.* **33**, 491–497.
- Moremen, K. W., Trimble, R. B. & Herscovics, A. (1994). *Glycobiology*, **4**(2), 113–125.
- Nguyen, M., Strubel, N. A. & Bischoff, J. (1993). *Nature (London)*, **365**, 267–269.
- Otwinowski, Z. & Minor, W. (1997). *Methods Enzymol.* **276**, 307–326.
- Sriramarao, P., Berger, E., Chambers, J. D., Arfors, K. E. & Gehlsen, K. R. (1993). *J. Cell. Biochem.* **51**(3), 360–368.